Strain modification in thin $Si_{1-x-y}Ge_xC_y$ alloys on (100) Si for formation of high density and uniformly sized quantum dots

Xiaoping Shao, Ralf Jonczyk, M. Dashiell, D. Hits, B. A. Orner, A.-S. Khan, K. Roe, J. Kolodzey, and Paul R. Berger[a)]
Department of Electrical and Computer Engineering, University of Delaware, Newark, Delaware 19716

M. Kaba and M. A. Barteau
Department of Chemical Engineering, University of Delaware, Newark, Delaware 19716

K. M. Unruh
Department of Physics and Astronomy, University of Delaware, Newark, Delaware 19716

(Received 26 May 1998; accepted for publication 21 September 1998)

The effects of alloying C with Ge and Si and varying the C/Ge ratio during the growth of very thin layers of the ternary alloy SiGeC grown on Si (100) substrates and the resulting strain modification on self-assembled and self-organized quantum dots are examined. During coherent islanded growth, where dislocations are not formed yet to relieve the strain, higher strain energy produced by greater lattice mismatch acts to reduce the island size, increase the density of islands, and significantly narrow the distribution of island sizes to nearly uniformly sized quantum dots. Strain energy can also control the critical thickness for dislocation generation within the three-dimensional islands, which then limits the maximum height which coherent islands can achieve. After the islands relax by misfit dislocations, the island sizes increase and the island size distribution becomes broader with the increase of misfit and strain. The optimal growth for a high density of uniform coherent islands occurred for the $Si_{0.49}Ge_{0.48}C_{0.03}$ alloy composition grown on (100) Si, at a growth temperature of 600 °C, with an average thickness of 5 nm, resulting in a narrow size distribution (about 42 nm diameter) and high density (about 2×10^{10} dots/cm^2) of quantum dots. © *1999 American Institute of Physics.* [S0021-8979(99)00801-4]

I. INTRODUCTION

Since the advent of molecular beam epitaxy over two decades ago, the growth of semiconductors with monolayer control has attracted enormous attention for quantum confined semiconductor structures.[1–3] Low dimensional structures have generated tremendous interest at many levels including the study of their fundamental physics as well as potentially important technological applications in electronic and optoelectronic devices due to their new electronic and optical properties. Currently there has been a tremendous commercial success in applications of quantum well based devices.[4] Quantum wires and quantum dots have numerous advantages over quantum wells. For example, quantum dots allow single charge counting and tunneling,[5–7] and the higher confinement modifies the density-of-states to significantly lower laser threshold currents and elevate differential gain. The fabrication of quantum wires and quantum dots with high densities and high uniformity, however, is difficult. Some experimental methods require complex and expensive lithography and processing. An alternative approach is self-organization by directly controlling the two-dimensional (2D) to 3D growth transition induced by lattice misfit stress. Studies on the surface morphology of heteroepitaxial films showed that the growth kinetics are strongly influenced by lattice mismatch induced strain energy, surface free energy, growth temperature, and growth rate.[8–10]

SiGe alloys seem to be a promising material system for realizing quantum dot structures for terabyte storage applications, since they can readily be implemented within existing Si technology. The growth of Ge on Si follows the Stranski–Krastanov mode of self-organized Ge-island formation when the epilayer thickness exceeds a few monolayers.[11–16] The addition of small amounts of C to SiGe acts to compensate in approximately a 1:8 ratio the compressive strain created by the addition of Ge to Si. This study examines alloying C with SiGe to form novel SiGeC quantum dots; the effects of subsequent strain modification on self-assembled and self-organized quantum dots are examined with improved control over strain.

II. EXPERIMENTAL PROCEDURES

A series of four $Si_{1-x-y}Ge_xC_y$ islanded samples were sequentially grown by the molecular beam epitaxy (MBE) technique in an EPI 620 solid source MBE system.[17,18] Silicon (100) wafers were prepared by chemically oxidizing the silicon surface using a solution of H_2O:H_2O_2:HCl (7:5:5), followed by dipping the wafers in a dilute hydrofluoric acid solution (10:1 H_2O:HF). After the HF dip, the samples were immediately loaded into the MBE load lock chamber to be pumped down to 1×10^{-8} Torr. The wafers were then trans-

a)Electronic mail: pberger@ee.udel.edu

TABLE I. Summary of growth parameters, calculated critical thicknesses and measured TEM and AFM parameters for the four $Si_{1-x-y}Ge_xC_y$ epilayers grown on (100) Si used in this study.

Composition	$Ge_{0.97}C_{0.03}$	$Si_{0.39}Ge_{0.58}C_{0.03}$	$Si_{0.49}Ge_{0.48}C_{0.03}$	$Si_{0.7}Ge_{0.27}C_{0.03}$
Sample ID	SGC224	SGC225	SGC226	SGC227
Growth time (min)	55	55	65	95
Epilayer thickness (Å)	50	50	50	50
Critical thickness (Å)	22	67	107	1735
Misfit (%)	4.0	1.4	1.0	0.1
No. of grains in 4×4 μm^2	77	2552	3171	1839
Grain size mean (nm^2)	2.5×10^4	1.9×10^3	1.4×10^3	4.3×10^3
Grain size diameter (nm)	178	49	42	74
Wavelength (μm/cycle)	0.5	0.078	0.068	0.085
Mean roughness (nm)	9.6	4.8	3.0	4.8
Peak relaxation misfit (%)	2.0	0.7	0.5	0.05
Modified crit. thickness in 3D island (Å)	40	162	248	3800
Island type	Relaxed	Relaxed	Coherent	Coherent

ferred into the growth chamber where they were prebaked at 200 °C following a procedure similar to that discussed in Eaglesham *et al.*[19] The prebake was shown to effectively desorb hydrocarbons on the Si surface which resulted in high quality Si epitaxy for substrate temperatures of $\geqslant$370 °C (defect densities $<10^5$ cm^{-2}). This step is necessary to avoid carbon contamination at the surface, which may act as nucleation sites for 3D growth. The samples were ramped to the growth temperature and the (2×1) reconstructed Si surface was confirmed by reflection high energy electron diffraction (RHEED). The substrate temperature during growth was held at 600 °C. The nominal film thickness for all the layers, assuming 2D growth, was 5 nm. Growth of the thin layers was performed without a buffer layer, but after RHEED confirmation of the (2×1) stabilized Si surface. The growth conditions maintained a nominal carbon composition of 3% for all of the four samples, while varying the Ge:Si ratio. The Si content was varied among 0%, 39%, 49%, and 70% (Table I), while the nominal C composition was held at 3%.

III. RESULTS AND DISCUSSION

The alloy composition of these epilayers was not measured directly, due to the very thin epitaxial layers employed here and the uneven step coverage. The alloy compositions were estimated from the growth conditions used, which were calibrated from Rutherford backscattering (RBS) measurements of thicker samples grown under similar conditions. A suitable method for measuring substitutional C in SiGeC alloys, without assuming Vegard's law holds, is to perform C resonant RBS. However, resonant RBS cannot measure alloy compositions below 1% C or thicknesses below ~1000 Å, and its error is ±0.2% above this threshold. Previous absorption measurements of $Si_{1-x}C_x$ and $Si_{1-x-y}Ge_xC_y$ layers monitoring the 810–815 cm^{-1} line associated with the vibration of coherent SiC precipitates and the 602–610 cm^{-1} line associated with the vibrational mode of substitutional C in Si have shown significant substitutional C for growth temperatures employed in this study.[20,21] Note the spread in the local vibrational mode energies due to the alloy effect with Ge.

The misfit dislocations at the substrate interface of these islands were examined with a Philips 400T transmission electron microscope (TEM), operating at 100 kV. Plan-view images were taken at the (220) Bragg reflection. Moiré fringes parallel to the (220) reflection plane were only found in the $Ge_{0.97}C_{0.03}$ sample (SGC224) and relatively large islands (diameter $\geqslant$50 nm) of the $Si_{0.39}Ge_{0.58}C_{0.03}$ sample (SGC225), indicating these islands are relaxed by interfacial misfit dislocations. No dislocations (or Moiré fringes) were observed in any islands for the $Si_{0.49}Ge_{0.48}C_{0.03}$ (SGC226) and $Si_{0.7}Ge_{0.27}C_{0.03}$ (SGC227) epilayers, and a strain contrast can be seen in both images, indicating that the islands in these two samples are coherently strained.

Atomic force microscopy (AFM) was used in the tapping mode to examine the surface morphology of each sample, and catalog the island size and distribution. Figure 1 shows typical AFM topographies from all four sample compositions: $Ge_{0.97}C_{0.03}$ (SGC224), $Si_{0.39}Ge_{0.58}C_{0.03}$ (SGC225), $Si_{0.49}Ge_{0.48}C_{0.03}$ (SGC226), and $Si_{0.7}Ge_{0.27}C_{0.03}$ (SGC227). The 3D island size distribution of these samples is also shown in histogram form (Fig. 1). Note that as the overall Si content increases, the misfit and strain energy is reduced, and AFM analysis shows that this acts to reduce the island size, increase the island density, and tighten the variation in island size, for the two relaxed islanded samples: SGC224 and SGC225. However, sample SGC226, with coherent islands, has the highest density of islands (about 2×10^{10} dots/cm^2), smallest island size (about 42 nm diameter), and the most uniform size distribution in this series. The sample with the largest Si content, $Si_{0.7}Ge_{0.27}C_{0.03}$ (SGC227) which also has coherent islands, shows an increased island size, a decreased island density, and a broader island size distribution, compared to SGC226. This trend is also observed in the power spectrum density analysis of the AFM data, shown in Fig. 2, which is the Fourier transform of the measured raw data, where the peaks shift to a smaller wavelength with increasing Si composition, but shifts back to larger wavelengths for the $Si_{0.7}Ge_{0.27}C_{0.03}$ sample. The changes in surface roughness with Si content can also be

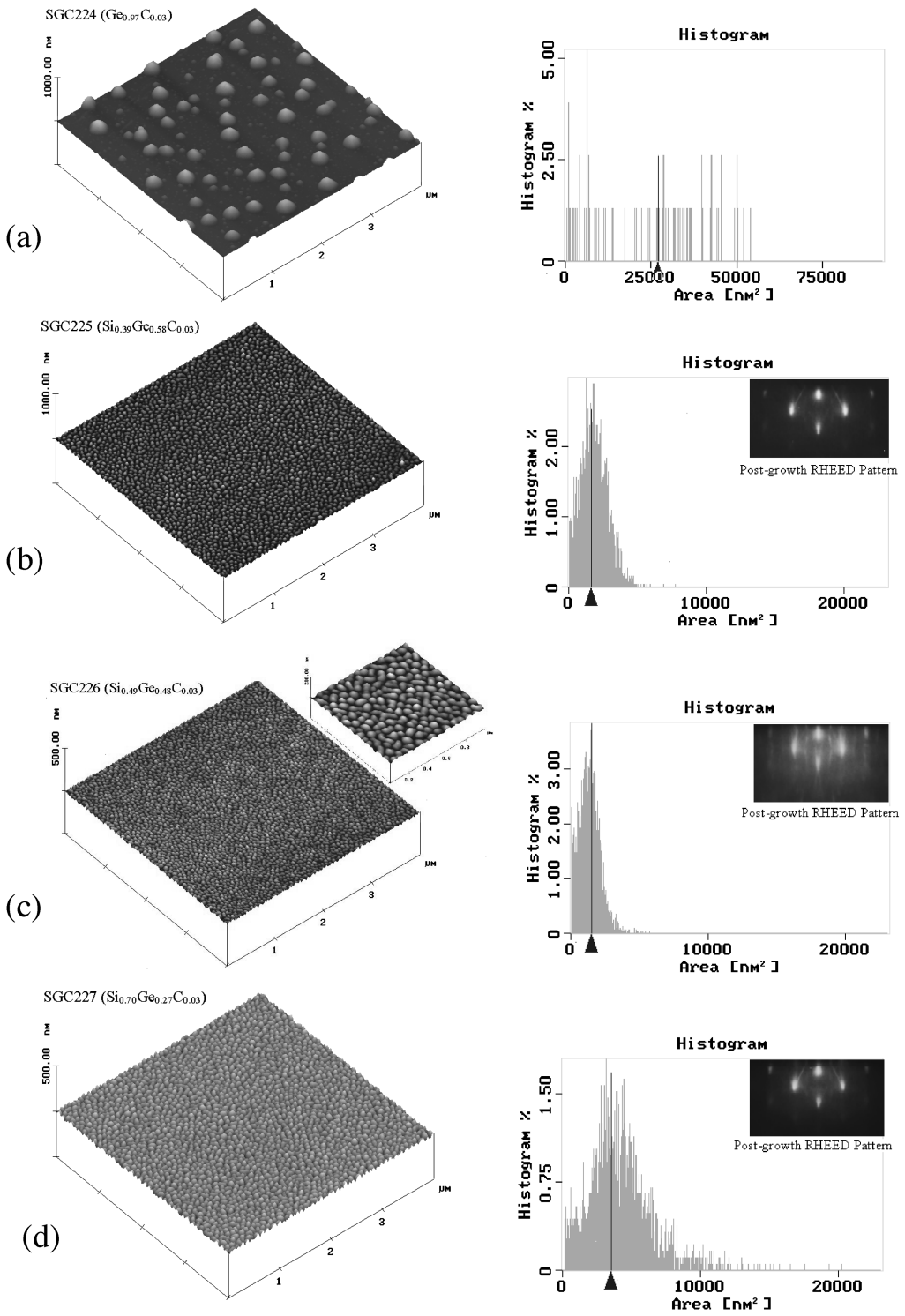

FIG. 1. AFM topographs of: (a) $Ge_{0.97}C_{0.03}$ (SGC224), (b) $Si_{0.39}Ge_{0.58}C_{0.03}$ (SGC225), (c) $Si_{0.49}Ge_{0.48}C_{0.03}$ (SGC226), and (d) $Si_{0.7}Ge_{0.27}C_{0.03}$ (SGC227), and their corresponding histograms, showing island size distribution. Insets show their corresponding postgrowth RHEED pattern.

seen from *in situ* reflection high-energy electron diffraction (RHEED), as shown in the insets in Figure 1.

Low temperature photoluminescence (PL) studies of all four layers are shown in Fig. 3. In all the layers a peak at 1.09 eV was observed which is related to the Si substrate. Narrow peaks are observed at 0.789 and 0.767 eV, as well as a broad band centered at 0.75 eV in the layers that contain silicon. They were found to increase in intensity with increasing Si content and decreasing Ge/C ratio. Very similar luminescence was observed by Wang *et al.*,[22] and was attributed to Ge no-phonon lines. However, studies of thermally induced defects in silicon by Minaev *et al.*[23] and Weber *et al.*[24] revealed luminescence at the same locations. They observed that electron–vibrational emission bands, *P* (0.767 eV), *H* (0.9258 eV), *T* (0.9356 eV) and *I* (0.9653 eV), found in *n*-type and *p*-type silicon caused thermally induced de-

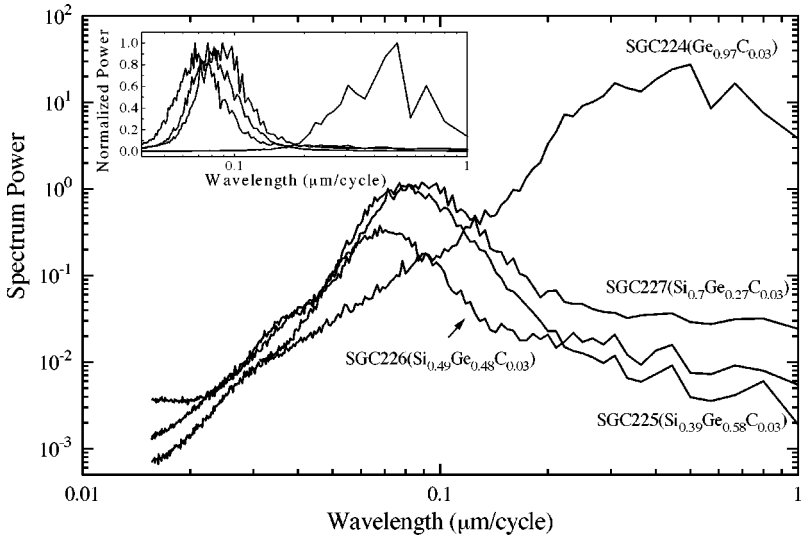

FIG. 2. Power spectrum density, showing Fourier spectral intensities of: $Ge_{0.97}C_{0.03}$ (SGC224), $Si_{0.39}Ge_{0.58}C_{0.03}$ (SGC225), $Si_{0.49}Ge_{0.48}C_{0.03}$ (SGC226), and $Si_{0.7}Ge_{0.27}C_{0.03}$ (SGC227), grown on (100) Si.

fects, incorporating oxygen and carbon impurity atoms. Additionally, they found the *P* line increased in intensity when the oxygen concentration was substantially larger than the carbon concentration. We attribute these PL lines in the SiGeC layers to thermally induced defects. The reason may be due to the thermal limitations on the Si effusion cell used in this study. Due to the ceramic crucible used for the Si source, the Si furnace cannot be raised too high in temperature. As a result, the epitaxial growth rate drops off considerably with increasing Si content. As the growth rate is reduced, the likelihood of impurity incorporation increases. For this reason, the oxygen contamination climbs with increasing Si content, and probably deleteriously affects the growth front of the last sample (SGC227), which is expected to exhibit a layer-by-layer 2D growth front with only a 0.1% misfit.

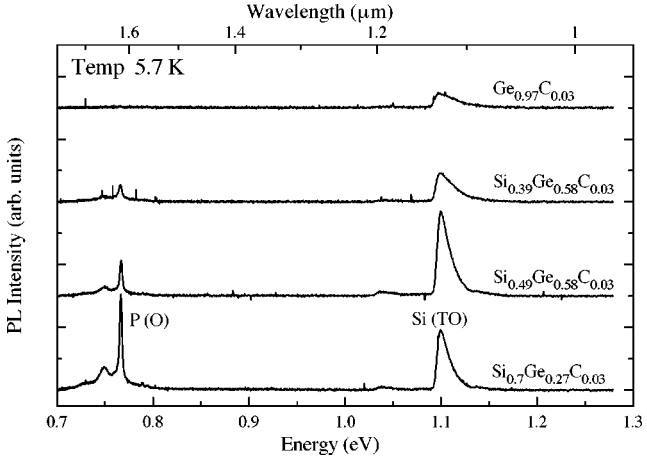

FIG. 3. Photoluminescence (PL) spectrum of: $Ge_{0.97}C_{0.03}$ (SGC224), $Si_{0.39}Ge_{0.58}C_{0.03}$ (SGC225), $Si_{0.49}Ge_{0.48}C_{0.03}$ (SGC226), and $Si_{0.7}Ge_{0.27}C_{0.03}$ (SGC227), grown on (100) Si. Note, the elevated *P* line due to impurity incorporation, notably, oxygen, as the growth rate is reduced for the higher concentrations of Si.

IV. CONCLUSIONS

Our results show that during coherent islanded growth, a larger Ge content, and therefore greater strain, can reduce the island size, increase island density, and narrow the island size distribution. Strain can also control the critical thickness for dislocation generation within 3D islands, which limits the maximum height that coherent islands can achieve. After relaxation by misfit dislocations, the island size increases and the island size distribution becomes broader with the decrease of Si content and increase of strain. In our case, the optimal growth for a high density of uniform coherent islands occurred for the composition of $Si_{0.49}Ge_{0.48}C_{0.03}$ on (100) Si, at a growth temperature of 600 °C, for an average thickness of 5 nm, resulting in a narrow size distribution (about 42 nm diameter) and high density (about 2×10^{10} dots/cm^2).

ACKNOWLEDGMENTS

The authors wish to express their thanks to Dr. Robert Hull of the University of Virginia for his fruitful discussions. This work was supported by the National Science Foundation (Grant No. ECS-9624160).

[1] A. Y. Cho and J. R. Arthur, Prog. Solid State Chem. **10**, 157 (1975).
[2] L. Esaki and L. L. Chang, Phys. Rev. Lett. **33**, 495 (1974).
[3] R. Dingle, W. Wiegmann, and C. H. Henry, Phys. Rev. Lett. **33**, 827 (1974).
[4] C. Weisbuch and B. Vinter, *Quantum Semiconductor Structures* (Academic, New York, 1991).
[5] D. A. Wharam, T. J. Thornton, R. Newbury, M. Pepper, H. Ahmed, J. E. Frost, D. G. Hasko, D. C. Peacock, and C. T. Foxon, J. Phys. C **21**, L209 (1988).
[6] A. Imamoglu and Y. Yamamoto, Phys. Rev. Lett. **72**, 210 (1994).
[7] *Single Charge Tunneling*, NATO Advanced Science Instrument Series B, edited by H. Grabert and M. H. Devoret (Plenum, New York, 1992).
[8] W. A. Jesser and J. H. van der Merwe, Surf. Sci. **31**, 229 (1972).
[9] P. R. Berger, K. Chang, P. Bhattacharya, J. Singh, and K. K. Bajaj, Appl. Phys. Lett. **53**, 684 (1988).
[10] J. Pamulapati, P. K. Bhattacharya, J. Singh, P. R. Berger, C. W. Snyder, B. G. Orr, and R. L. Tober, J. Electron. Mater. **25**, 479 (1996).

[11] H. Sunamura, N. Usami, Y. Shiraki, and S. Fukatsu, Appl. Phys. Lett. **66**, 3024 (1995).
[12] P. Schittenhelm, M. Gail, J. Brunner, J. F. Nützel, and G. Abstreiter, Appl. Phys. Lett. **67**, 1292 (1995).
[13] E. Palange, G. Capellini, L. DiGaspare, and F. Evangelisti, Appl. Phys. Lett. **68**, 2982 (1996).
[14] M. Krishnamurthy, B.-K. Yang, and W. H. Weber, Appl. Phys. Lett. **69**, 2572 (1996).
[15] O. G. Schmidt, C. Lange, K. Eberl, O. Kienzle, and F. Ernst, Appl. Phys. Lett. **71**, 2340 (1997).
[16] R. Jonczyk, D. A. Hits, L. V. Kulik, J. Kolodzey, M. Kaba, and M. A. Barteau, J. Vac. Sci. Technol. B **16**, 1142 (1998).
[17] J. Kolodzey *et al.*, J. Cryst. Growth **157**, 386 (1995).
[18] J. Kolodzey, P. A. O'Neil, S. Zhang, B. A. Orner, K. Roe, K. M. Unruh, C. P. Swann, M. M. Waite, and S. Ismat Shah, Appl. Phys. Lett. **67**, 1865 (1995).
[19] D. J. Eaglesham, G. S. Higashi, and M. Cerullo, Appl. Phys. Lett. **59**, 685 (1991).
[20] M. W. Dashiell, L. V. Kulik, D. Hits, J. Kolodzey, and G. Watson, Appl. Phys. Lett. **72**, 833 (1998).
[21] L. V. Kulik, D. A. Hits, M. W. Dashiell, and J. Kolodzey, Appl. Phys. Lett. **72**, 1972 (1998).
[22] X. Wang, Z. Jiang, H. Zhu, F. Lu, D. Huang, X. Liu, C. Hu, Y. Chen, Z. Zhu, and T. Yao, Appl. Phys. Lett. **71**, 3543 (1997).
[23] N. S. Minaev and A. V. Mudryi, Phys. Status Solidi A **68**, 561 (1981).
[24] J. Weber and R. Sauer, Mater. Res. Soc. Symp. Proc. **14**, 165 (1983).